Adaptive Evolution of 3D Curves for Quality Control

H. Martinsson, F. Gaspard
CEA, LIST, Boîte Courrier 94, F-91 191 Gif sur Yvette, France;
tel: +33(0)1 69 08 82 98, fax: +33(0)1 69 08 83 95
hanna.martinsson@cea.fr
A. Bartoli, J.-M. Lavest
LASMEA (CNRS/UBP), 24 avenue des Landais, F-63 177 Aubière, France;
tel: +33(0)4 73 40 76 61, fax: +33(0)4 73 40 72 62
adrien.bartoli@gmail.com

Abstract – **In the area of quality control by vision, the reconstruction of 3D curves is a convenient tool to detect and quantify possible anomalies. Whereas other methods exist that allow us to describe surface elements, the contour approach will prove to be useful to reconstruct the object close to discontinuities, such as holes or edges.**

We present an algorithm for the reconstruction of 3D parametric curves, based on a fixed complexity model, embedded in an iterative framework of control point insertion. The successive increase of degrees of freedom provides for a good precision while avoiding to over-parameterize the model. The curve is reconstructed by adapting the projections of a 3D NURBS snake to the observed curves in a multi-view setting. The sampling of the curve is adjusted as a function of the local visibility in the different views. The optimization of the curve is performed with respect to the control points using an gradient-based energy minimization method, whereas the insertion procedure relies on the computation of the distance from the curve to the image edges.

Keywords – **Active Contours, Curve Reconstruction, Quality Control, Multi-View**

I. Introduction

The use of optical sensors in metrology applications is a complicated task when dealing with complex or irregular structures. More precisely, projection of structured light allows for an accurate reconstruction of surface points but does not allow for a precise localization of the discontinuities of the object. This paper deals with the problem of reconstruction of 3D curves, given the CAD model, for the purpose of a control of conformity with respect to this model. We dispose of a set of images with given perspective projection matrices. The reconstruction will be accomplished by means of the observed contours and their matching, both across the images and to the model. We proposed a previous version of our algorithm, based on edge distances, in [1]. The contributions of this paper with respect to the former one resides in the energy formulation, giving a new structure to the problem. We have also introduced an adaptive sampling method and completed the experimental evaluation.

Algorithms based on active contours [2] allows for a local adjustment of the model and a precise reconstruction of primitives. More precisely, the method allows for an evolution of the reprojected model curves toward the image edges, thus to minimize the distance in the images between the predicted curves and the observed edges.

The parameterization of the curves as well as the optimization algorithms we use must yield an estimate that meets the requirements of accuracy and robustness necessary to perform a control of conformity. We have chosen to use NURBS curves [3], a powerful mathematical tool that is also widely used in industrial applications.

In order to ensure stability, any method used ought to be robust to erroneous data, namely the primitives extracted from the images, since images of metallic objects incorporate numerous false edges due to reflections.

Although initially defined for ordered point clouds, active contours have been adapted to parametric curves. Cham and Cipolla propose a method based on affine epipolar geometry [4] that reconstructs a parametric curve in a canonical frame using stereo vision. The result is

two coupled snakes, but without directly expressing the 3D points. In [5], Xiao and Li deal with the problem of reconstruction of 3D curves from two images. However, the NURBS curves are approximated by B-splines, which makes the problem linear, at the expense of loosing projective invariance. The reconstruction is based on a matching process using epipolar geometry followed by triangulation. The estimation of the curves is performed independently in the two images, that is, there is no interactivity between the 2D observations and the 3D curve in the optimization.

In the field of medical imaging, energy minimization methods have been developed to reconstruct 3D curves in a stereo setting. Sbert and Solé reconstruct in [6] a 3D curve using an energy based evolution method. The associated PDE of the energy functional, derived by the Euler-Lagrange formulation, is solved using a level-set approach. In [7], Canero et al. define in a force field by reprojecting external image forces, given by the distance to the edges. A 3D curve is then reconstructed via the evolution of an active contour, guided by the force field.

In the case of 2D curve estimation, other aspects of the problem are addressed. Cham and Cipolla adjust a spline curve to fit an image contour [8]. Control points are inserted iteratively using a new method called PERM (potential for energy-reduction maximization). An MDL (minimal description length [9]) strategy is used to define a stopping criterion. In order to update the curve, the actual curve is sampled and a line-search is performed in the image to localize the target shape. The optimization is performed by gradient descent. Brigger et al. present in [10] a B-spline snake method without internal energy, due to the intrinsic regularity of B-spline curves. The optimization is done on the knot points rather than on the control points, which allows the formulation of a system of equations that can be solved by digital filtering. So as to increase numerical stability, the method is embedded in a multi-resolution framework. In [11], Figueiredo et al. address the problem from a statistical point of view, proposing a completely automatic contour estimator, in the sense that no parameter need to be adjusted by the user. Supposing a uniform distribution of the knot points, the B-spline curve that approximates a given set of contour points at best, in the least squares sense, is given by a linear system depending only on the number of control points. This number is fixed in advance using an MDL criterion. Meegama and Rajapakse introduce in [12] an adaptive procedure for control point insertion and deletion, based on the euclidean distance between consecutive control points and on the curvature of the NURBS curve. Local control is ensured by adjustment of the weights. The control points evolve in each iteration in a small neighborhood (3×3 pixels).

Despite the numerous approaches found in the literature, we are not aware of any 3D reconstruction method using parametric active contours in 3D, based on several images, with an adaptive complexity. For our metrology applications, in order to obtain a very high precision, we need an a priori knowledge of the camera parameters as well as a good initialization of the curve. It is in this context we present our method.

II. Problem Formulation

Given a set of images of an object, together with its CAD model, our goal is to reconstruct in 3D the curves observed in the images, by minimizing an energy functional. In order to obtain a 3D curve that meets our requirements regarding regularity, rather than reconstructing a point cloud, we estimate a NURBS curve. Since the regularity aspects are thereby taken care of, the energy functional is defined solely based on image data. The minimization problem is formulated for a set of M images and N sample points by

$$\mathbf{C}(\mathcal{P}) = \arg\min_{\mathcal{P}} \sum_{i=0}^{M-1} \sum_{j=0}^{N-1} E(T_i(\mathbf{C}(\mathcal{P}, t_j))), \tag{1}$$

where E is the external energy functional, T_i is the projective operator for image i and $\mathcal{P}$ is the set of control points.

Our choice to use NURBS curves is justified by several reasons. First, NURBS curves have interesting geometrical properties, namely concerning regularity and continuity. An important geometrical property that will be of particular interest is the invariance under projective transformations.

III. Properties of NURBS curves

Let $U = \{u_0, \cdots, u_m\}$ be an increasing vector, called the knot vector. A NURBS curve is a vector valued, piecewise rational polynomial over U, defined by

$$\mathbf{C}(t) = \sum_{i=0}^{n} \mathbf{P}_i R_{i,k}(t) \quad \text{with} \quad R_{i,k}(t) = \frac{w_i B_{i,k}(t)}{\sum_{j=0}^{n} w_j B_{j,k}(t)}, \tag{2}$$

where $\mathbf{P}_i$ are the control points, $B_{i,k}(t)$ the B-spline basis functions defined over U, w_i the associated weights and k the degree. The name NURBS (Non-Uniform Rational B-Splines) indicates that the knot vector is non-uniform, that is, the knot points are not equi-distant, and that the pieces of the curve are rational polynomials.

It is a common choice to take $k = 3$, which has proved to be a good compromise between required smoothness and the problem of oscillation, inherent to high degree polynomials. Given all these parameters, the set of NURBS defined on U forms, together with the operations of point-wise addition and multiplication with a scalar, a vector space.

For details on NURBS curves and their properties, refer to [3].

A. Projective Invariance

According to the pinhole camera model, the perspective projection $T(\cdot)$ that transforms a world point into an image point is expressed in homogeneous coordinates by means of the transformation matrix $\mathbf{T}_{3\times4}$. Using weights associated with the control points, NURBS curves have the important property of being invariant under projective transformations. Indeed, the projection of (2) remains a NURBS, defined by its projected control points and their modified weights. The curve is written

$$\mathbf{c}(t) = T(\mathbf{C})(t) = \frac{\sum_{i=0}^{n} w_i' \, T(\mathbf{P}_i) \, B_{i,k}(t)}{\sum_{i=0}^{n} w_i' \, B_{i,k}(t)} = \sum_{i=0}^{n} T(\mathbf{P}_i) R_{i,k}'(t), \tag{3}$$

where the $R_{i,k}'$ are the basis functions of the projected NURBS. The new weights, w_i', are given by

$$\begin{aligned} w_i' &= (T_{3,1}X_i + T_{3,2}Y_i + T_{3,3}Z_i + T_{3,4})\, w_i \\ &= \mathbf{n} \cdot (\mathbf{C}_\mathrm{O} - \mathbf{P}_i)\, w_i, \end{aligned} \tag{4}$$

where $\mathbf{n}$ is a unit vector along the optical axis and $\mathbf{C}_\mathrm{O}$ the optical center of the camera.

B. Control Point Insertion

One of the fundamental geometric algorithms available for NURBS curves is the control point insertion. The key is the knot insertion, which is equivalent to adding one dimension to the vector space, consequently adapting the basis. Since the original vector space is included in the new one, there is a set of control points such that the curve remains unchanged. Note that only k new control points need to be computed, due to the local influence of splines.

IV. Optimization

When treating NURBS curves, the regularity aspects are taken care of implicitly by the parameterization and the energy functional can be reduced to its external energy part. We will consider two forms of energy functionals, one based on the distance from the curve to the image contours and another one based on the gradient intensity. The optimization will in both cases operate on the control points of the 3D NURBS curve.

A. Distance Minimization

Using a distance formulation and the properties of NURBS curves, the minimization problem (1) is written

$$\min_{\{\hat{\mathbf{P}}_l\}} \sum_{i=0}^{M-1} \sum_{j=0}^{N-1} \left(\mathbf{q}_{ij} - \sum_{l=0}^{n} T_i(\hat{\mathbf{P}}_l) R_{l,k}^{(i)}(t_j) \right)^2, \tag{5}$$

where $\mathbf{q}_{ij}$ is a contour point associated with the curve point of parameter t_j in image i and T_i is the projective operator for image i.

Search for Image Contours

We sample the NURBS curve projected in the image, to use as starting points in the search for matching contour points. A line-search is performed in order to find the new position of the curve, ideally corresponding to an edge. Our approach is based solely on the contours. Due to the aperture problem, the component of motion of an edge, tangent to itself, is not detectable locally and we therefore restrict the search for the new edge position to the edge normal. As we expect the motion to be small, to limit computational cost, we define a search range. In order to find the new position of a sample point, for each point belonging to the normal within the range, we evaluate the gradient and compute a weight based on the intensity and the orientation of the gradient and the distance from the sample point. The weight function will be evaluated for each candidate and the point p_j' with the highest weight, identified by its distance from the original point, will be retained as the candidate for the new position of the point.

The bounded search range and the weighting of the point based on their distance from the curve yield a robust behavior, close to that of an M-estimator.

B. Gradient Energy Minimization

Using the classical energy formulation and the properties of NURBS curves, the minimization problem (1) can be written

$$\min_{\{\hat{\mathbf{P}}_l\}} \sum_{i=0}^{M-1} \sum_{j=0}^{N-1} E\left(\sum_{l=0}^{n} T_i(\hat{\mathbf{P}}_l) R_{l,k}^{(i)}(t_j) \right), \tag{6}$$

where $R_{l,k}^{(i)}$ are the basis functions for the projected NURBS curve in image i. The energy functional E can, as already mentioned, be restricted to its external part, due to the use of NURBS. A common choice is to use the gradient intensity. We will however include local information on the curve, namely its normal direction, using the intensity of the gradient projected onto the curve normal.

C. Distance versus Gradient Energy

For comparison, we have implemented the two methods in the iterative setting that will be introduced in the following section. Both methods yielded similar results and converge after a number of iterations to an asymptotic lower limit. The 3D error with respect to the true curve is however somewhat lower for the gradient-based method. The results are given in Fig. 1. The difference is partly explained by the noise and the parallel structures perturbing the edge tracking algorithm. An example of candidate points located on a parallel image contour, due to specularities, is given in Fig. 2. Although the gradient intensity method outperforms the distance method, the distance-based cost function will prove to be useful in the iterative framework that will embed the curve optimization.

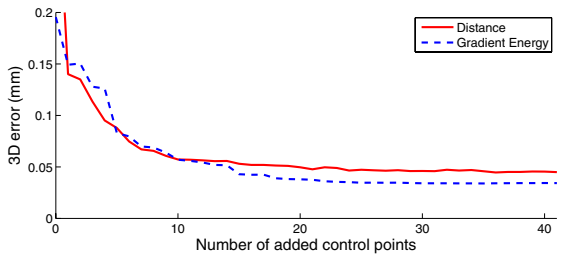

Fig. 1. The evolution of the error, with respect to the true 3D curve, for an optimization using cost functions based on the distance to the image contours and on the gradient intensity respectively.

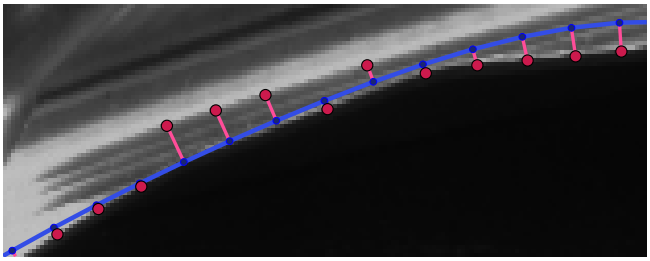

Fig. 2. Problems related to specularities and to the search for candidate points. The initial curve and candidate points.

V. Curve Estimation

The problem has two parts. First, the optimization of the 3D NURBS curve by energy minimization on a fixed number of control points, then the control point insertion procedure. For the fixed size optimization problem, we use the non-linear Levenberg-Marquardt minimization method. This step allows the control points to move in 3D, but does not change their number. In order to obtain an optimal reconstruction of the observed curve, we iteratively perform control point insertion. So as to avoid over-parameterization for stability reasons, the first optimization is carried out on a limited number of control points. Their number is then increased by iterative insertion, so that the estimated 3D curve fits correctly also in high curvature regions. As mentioned earlier, the insertion of a control point is done without influence on the curve and a second optimization is thus necessary in order to take advantage from the increased number of degrees of freedom.

A. Optimization on the Control Points

The first step of the optimization consists in projecting the curve in the images. Since the surface model is known, we can identify the visible parts of the curve in each image and retain only the sample points corresponding to visible parts. During the iterations, to keep the same cost function, the residual error must be evaluated in the same points in each iteration. Supposing small displacements, we can consider that visible pieces will remain visible throughout the optimization.

The optimization of (6) is done on the 3D control point coordinates, leaving the remaining parameters of the NURBS curve constant. The weights associated with the control points are modified by the projection giving 2D weights varying with the depth of each control point, according to the formula (4), but they are not subject to the optimization.

B. Control Point Insertion

Due to the use of NURBS, we have a method to insert control points. What remains is to decide where to place them. We also need a criterion to decide when to stop the control point insertion procedure.

Position of the New Control Point

Several strategies have been used. Cham and Cipolla consider in [8] the dual problem of knot insertion. They define an error energy reduction potential and propose to place the knot point so as to maximize this potential. The control point is placed using the method described earlier. In our algorithm, since every insertion is followed by an optimization that adjusts the control points, we settle for choosing the interval where to place the point. Since the exact location within the interval is not critical, the point is placed at its midpoint. Dierckx suggests in [13] to place the new point at the interval that presents the highest error. This is consistent with an interpretation of the error as the result of a lack of degrees of freedom that inhibits a good description of the curve. If, however, the error derives from other sources, this solution is not always optimal.

In our case, a significant mean error could also indicate the presence of parasite edges or that of a parallel structure close to the target curve. We will therefore choose the interval with the highest median error, over all images. The error is defined as the distance from a sample point to its corresponding contour point in the image. The search for candidate contour points is carried out using the method described in A.

Stopping Criterion

One of the motives for introducing parametric curves was to avoid treating all curve points, as only the control points are modified during the optimization. If the number of control points is close to the number of samples, the benefit is limited. Too many control points could also cause numerical instabilities, due to an over-parameterization of the curve on the one hand and the size of the non-linear minimization problem on the other hand. It is thus necessary to define a criterion that decides when to stop the control point insertion.

A strategy that aims to avoid the over-parameterization is the use of statistical methods inspired by the information theory. Based in a Maximum Likelihood environment, these methods combine a term equivalent, in the case of a normal distributed errors, to the sum of squares of the

residual errors with a term penalizing the model complexity. Given two estimated models, in our case differentiated by their number of control points, the one with the lowest criterion will be retained. A criterion of this type, based on a bayesian formalism, is the BIC (Bayesian Information Criterion) presented by Schwarz [14]. It stresses the number of data points n, so as to ensure an asymptotic consistency and is written, in the case of normally distributed errors,

$$BIC = 2k \ln n + n \ln \frac{RSS}{n}, \tag{7}$$

where k is the number of control points and RSS is the sum of the squared residual errors.

Another family of methods uses the MDL [15] formulation, which consists in associating a cost with the quantity of information necessary to describe the curve. Different criteria follow, depending on the formulation of the estimation problem. In the iterative control point insertion procedure of Cham et Cipolla [8], the stopping criterion is defined by means of MDL. The criterion depends, on the one hand on the number of control points and on the residual errors, on the other hand on the number of samples and on the covariance.

We have chosen to use the BIC, computed using the contour points found with the method presented in A, for this first version of our algorithm. A more thorough study of the influence of the stopping criterion in our setting will be performed at a later stage.

Adaptive Sampling

Each new control point adds an interval to the curve. In order to increase the resolution in regions where the curve undergoes changes rather than globally, the sampling follows the intervals. The insertion of a control point also increases the number of sample points. Furthermore, the sampling is adapted to the visibility of the interval in the images. The number of samples is thus based on the projected length of the interval and not on the length of the interval on the 3D curve. Each 2D curve is sampled separately per interval, with a lower limit on the mean distance between sample points of one pixel. This is to avoid giving too much weight to barely visible intervals.

C. Algorithm

The algorithm we implemented has two layers. The optimization of a curve using a fixed complexity model is embedded in an iterative structure that aims to increase the number of control points. The non-linear optimization of the 3D curve is performed by the Levenberg-Marquardt algorithm, using a cost function based on an energy formulation. The control point insertion procedure uses a search for contour points in the images in order to compute the median as well as the RSS error of the projected curve.

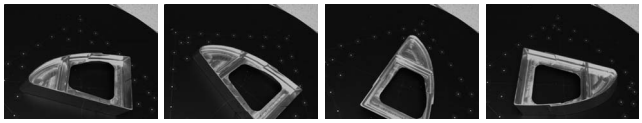

Fig. 3. Some of the 36 real images used for the reconstruction of the curve describing the central hole.

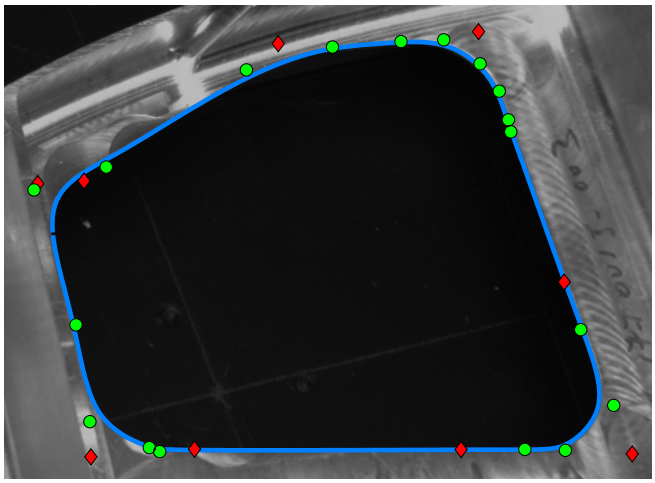

Fig. 4. Evolution of the control points. The figure shows the 10 initial control points (diamonds), the 18 control points after optimization (circles) and the final curve.

VI. Experimental Evaluation

A. Real Images

We consider a set of images, see Fig. 3, with a single target curve, using a modified "model curve". We now need to face the problem of noisy image data, multiple parallel structures and imprecision in the localization and the calibration of the views. The image size is 1392×1040 pixels. The starting curve has 10 control points, to which 8 new points are added. The initial sampling used for the computations is of 200 points. At the mean distance from the object curve, one pixel corresponds roughly to 0.28 mm. The distances from the target curve are shown in Fig. 3. We obtain the following results:

Mean error	0.115 mm
Median error	0.099 mm
Standard deviation	0.076 mm

The evolution of the control points is demonstrated in Fig. 4, where the set of initial control points is shown, together with the final curve and its control points. As expected, the control points inserted are concentrated in the regions of high curvature, such as the corners. We note that the error corresponds to less than a pixel in the images, which indicates a sub-pixel image precision. The error is explained by the noise and to some extent by specularities, causing parallel structures perturbing the minimization algorithm, see Fig. 5.

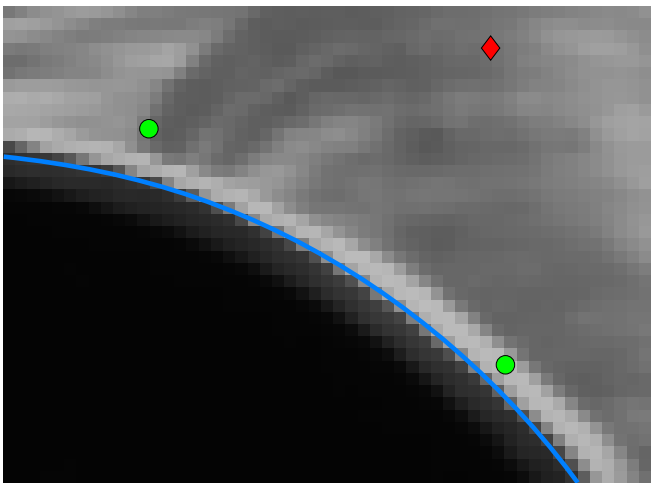

Fig. 5. A detail, showing the curve between two similar contours, the parallel model curve to the lower left and a false edge caused by specularities to the upper right.

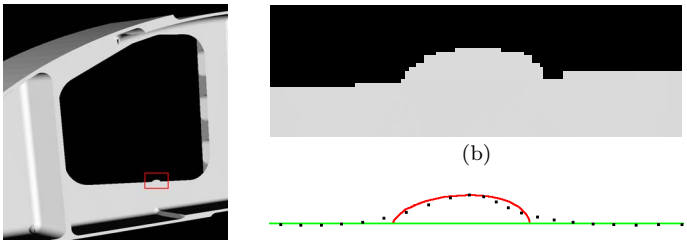

Fig. 6. Reconstruction of a nonconformity based on a series of virtual images of an object with an anomaly. The object is shown in (a), with a close-up in (b). The result of the reconstruction around the anomaly is shown in (c), with the original curve being a straight line and the reconstructed points matching the anomaly in black.

B. Virtual Images

As we do not dispose of an object presenting an anomaly, we have simulated deformations of the target object. Using a series of virtual images of an object presenting a minor anomaly, we have tested the capacity of our system to detect nonconformities, see Fig. 6. Based on 27 images and starting at the model curve, our algorithm manages to reconstruct the curve and its anomaly with a mean error of 0.0765 mm. Although the reconstruction is good, the error is concentrated around the anomaly, which is somewhat smoothed out.

VII. Conclusions

We have presented an adaptive 3D reconstruction method using parametric curves, limiting the degrees of freedom of the problem. An algorithm for 3D reconstruction of curves using a fixed complexity model is embedded in an iterative framework, allowing an enhanced approximation by control point insertion. The optimization of the curve with respect to the control points is performed by means of a minimization of an gradient-based energy functional, whereas the insertion procedure is based on the distance from the curve to the observed image contours. In order to use at best the information contained in the images, the sampling is adapted to the local visibility of the curve in the different images. An experimental evaluation of the method, using real as well as virtual images, has let us validate its performance in some simple, nevertheless realistic, cases with specular objects subject to occlusions, noise and deformations.

Future work will be devoted to the integration of the knowledge of the CAD model in the image based edge tracking. Considering the expected neighborhood of a sample point, the problem of parasite contours should be controlled and thus have limited impact on the obtained precision.

References

[1] H. Martinsson, F. Gaspard, A. Bartoli, and J-M. Lavest, "Reconstruction of 3d curves for quality control," in *15th Scandinavian Conference on Image Analysis*, 2007 (to appear).

[2] M. Kass, A. Witkin, and D. Terzopoulos, "Snakes: Active contour models," *International Journal of Computer Vision*, vol. 4, no. 1, pp. 321–331, 1987.

[3] L. Piegl and W. Tiller, *The NURBS book*, Monographs in visual communication. Springer Verlag, 2nd edition, 1997.

[4] T.-J. Cham and R. Cipolla, "Stereo coupled active contours," in *Conference on Computer Vision and Pattern Recognition*. IEEE Computer Society, 1997, pp. 1094–1099.

[5] Y.J. Xiao and Y.F. Li, "Stereo vision based on perspective invariance of NURBS curves," in *IEEE International Conference on Mechatronics and Machine Vision in Practice*, 2001, vol. 2, pp. 51–56.

[6] C. Sbert and A.F. Solé, "Stereo reconstruction of 3d curves," in *15th International Conference on Pattern Recognition (ICPR'00)*, 2000, vol. 1.

[7] C. Canero, P. Radeva, R. Toledo, J.J. Villanueva, and J. Mauri, "3D curve reconstruction by biplane snakes," in *15th International Conference on Pattern Recognition (ICPR'00)*, 2000, vol. 4, pp. 563–566.

[8] T.-J. Cham and R. Cipolla, "Automated B-spline curve representation incorporating MDL and error-minimizing control point insertion strategies," *IEEE Transactions on Pattern Analysis and Machine Intelligence*, vol. 21, no. 1, pp. 49–53, January 1999.

[9] M. H. Hansen and B. Yu, "Model selection and the principle of minimum description length," *Journal of the American Statistical Association*, vol. 96, no. 454, pp. 746–774, 2001.

[10] P. Brigger, J. Hoeg, and M. Unser, "B-spline snakes: A flexible tool for parametric contour detection," *IEEE Trans. on Image Processing*, vol. 9, no. 9, pp. 1484–1496, July 2000.

[11] M. Figueiredo, J. Leitão, and A.K. Jain, "Unsupervised contour representation and estimation using B-splines and a minimum description length criterion," *IEEE Transactions on Image Processing*, vol. 9, no. 6, pp. 1075–1087, June 2000.

[12] R.G.N. Meegama and J. C. Rajapakse, "NURBS snakes," *Image and Vision Computing*, vol. 21, pp. 551–562, 2003.

[13] P. Dierckx, *Curve and Surface Fitting with Splines*, Oxford University Press, Inc., New York, NY, USA, 1993.

[14] G. Schwarz, "Estimating the dimension of a model," *Ann. of Stat.*, vol. 6, pp. 461–464, 1978.

[15] J. Rissanen, "Modeling by shortest data description," *Automatica*, vol. 14, pp. 465–471, 1978.